

Massively Parallel Path Space Filtering

Nikolaus Binder
NVIDIA

Sascha Fricke
University of Braunschweig

Alexander Keller
NVIDIA



Figure 1: Path tracing at one path per pixel (left) in combination with hashed path space filtering (middle) very closely approximates the reference solution using 1024 paths per pixel (right). The filtering takes about 1.5 ms in HD resolution. Scene credit: Amazon Lumberyard Bistro, Open Research Content Archive [8].

ABSTRACT

Restricting path tracing to a small number of paths per pixel for performance reasons rarely achieves a satisfactory image quality for scenes of interest. However, path space filtering may dramatically improve the visual quality by sharing information across vertices of paths classified as proximate. Unlike screen space-based approaches, these paths neither need to be present on the screen, nor is filtering restricted to the first intersection with the scene. While searching proximate vertices had been more expensive than filtering in screen space, we greatly improve over this performance penalty by storing and looking up the required information in a hash table. The keys are constructed from jittered and quantized information, such that only a single query very likely replaces costly neighborhood searches. A massively parallel implementation of the algorithm is demonstrated on a GPU.

1 INTRODUCTION

Realistic image synthesis consists of high-dimensional numerical integration of functions with potentially high variance. Restricting the number of samples therefore often results in visible noise, which efficiently can be reduced by path space filtering [7] as shown in Figures 1 and 9.

We improve the performance of path space filtering by replacing costly neighborhood search with averages of clusters resulting from quantization. Our new algorithm is suitable for interactive and even real-time rendering and it enables many applications trading a controllable bias for a dramatic speedup and noise reduction.

2 PREVIOUS WORK

Filtering results of light transport simulation is gaining more and more attention in real-time, interactive, and even offline rendering. The surveys by Zwicker et al. [13] and Sen et al. [12] present an overview of recent developments. The fastest approaches use only information available at primary intersections and perform filtering in screen space. Further recent work is based on deep neural

networks [1, 2], hierarchical filtering with weights based on estimated variance in screen space [11] or on improving performance by simplifying the overall procedure [9].

Path space filtering [7], on the other hand, averages contributions of light transport paths in path space, which allows for filtering at non-primary intersections and for a more efficient handling of dis-occlusions during temporal filtering. However, querying the contributions in path space so far had been significantly more expensive than filtering the contributions of neighboring pixels in screen space. Neglecting the fact that locations that are close in path space are not necessarily adjacent in screen space enables interactive filtering in screen space [4]. As a consequence, filtering is almost only a good approximation for primary rays. In fact, such filtering algorithms are a variant of a bilateral filtering using path space proximity to determine weights.

Fast filtering is also possible in texture space [10], which at least requires a bijection between the scene surface and texture space. While this may be tricky already, issues may arise along discontinuities of a parametrization in addition.

Querying hash tables of sufficiently large size often requires only a single memory access, resulting in a constant complexity most of the time. Hence costly neighborhood search may be replaced by accumulating contributions with identical hashes of quantized path space descriptors, which is core to the proposed method.

3 ALGORITHM

The new scheme consists of three major steps as illustrated in Figure 2: After a set of light transport paths has been generated, for example by a path tracer, a key is constructed for each one selected vertex of each path. This key incorporates all information required to cluster proximate vertices: All contributions with identical hashes are atomically added. The number of contributions per hash is maintained by an atomic counter, too, and used to finally compute the average contribution. For each path its associated average is multiplied by its throughput and accumulated in its respective pixel. The throughput is the attenuation from the camera along the

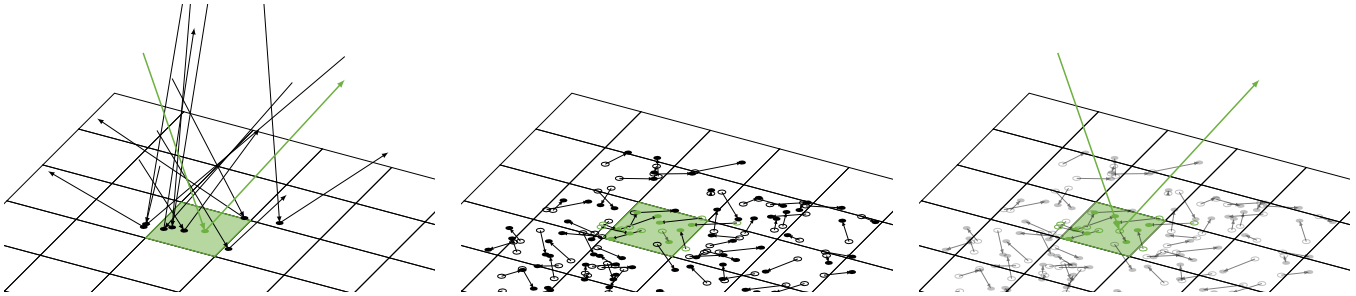


Figure 2: Illustration of the algorithmic principle in two dimensions: In order to determine the filtered contribution for the exemplary vertex along the green path segment, all selected vertices (left) are jittered by vectors sampled proportional to a filter kernel density (middle). Then the displaced vertices are quantized according to the underlying grid. Finally, all contributions with their hash identical to the hash of the vertex of interest are averaged (right). Note that in the general case the grid may not be aligned to the plane of jittering directions, see Figure 5.

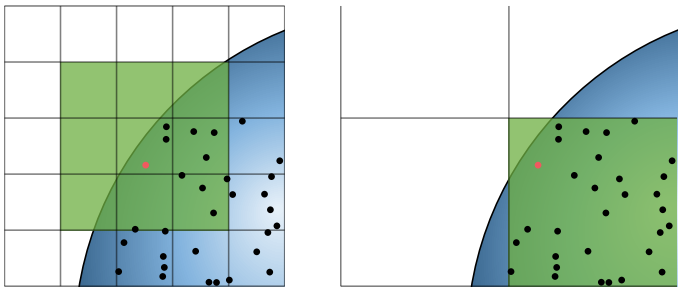


Figure 3: Instead of searching the n^3 neighborhood (left), we use the clustering resulting from quantization to accumulate contributions, which allows for a single look up (right).

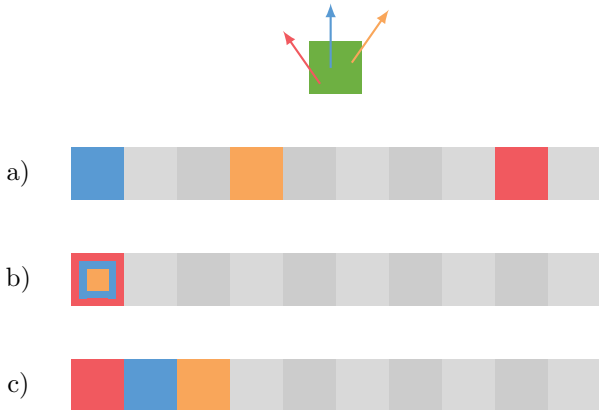


Figure 4: Instead of including normals in the descriptor a) to differentiate contributions whose vertices fall into the same cluster b), the verification hash function can be applied to a descriptor including normal information. This allows one to differentiate normal information by linear probing as shown in c).

light transport path up to the selected vertex, for example, the first sufficiently diffuse vertex [7].

3.1 Hashing Quantized Descriptors

Other than neighborhood search, hashing allows for sorting and searching in linear time. We therefore apply a fast hash function to a key, which is the descriptor of a path, and accumulate the contributions of all light transport paths with identical hash, see Figure 3.

A descriptor contains at least the quantized world space position of a selected vertex of a light transport path. As shown in Algorithm 1, level of detail can efficiently be handled by the descriptor, too: A heuristic as simple as the distance d along the path is sufficient to select a level of detail for accumulation. Adding information about the normal in that location avoids blurring lighting across edges. Furthermore the incoming direction for non-diffuse materials and the layer identifier for layered materials may be included in the descriptor.

Instead of storing and comparing the rather long descriptors for hash verification, we apply a second, different hash function to the same descriptor and accumulate a contribution only if the secondary hashes v match, see Algorithm 1. In order to increase the occupancy in the hash table, linear probing with a very small number of steps is employed when encountering a hash collision. Restricting linear probing to stay within one cache line, the collision resolution is almost negligible on modern architectures. Unless a hash collision can be resolved, we resort to the unfiltered original contribution of the path.

In addition, linear probing may be used to differentiate attributes of the light transport path at a finer level of detail as shown in Figure 4: For example, normal information may be included in the descriptor handed to the verification hash function instead of already including it in the main descriptor. This allows one to search for similar normals by linear probing.

3.2 Filter Kernel Approximation by Jittering

The discontinuities of quantization are removed by jittering key parameters in the path descriptor, which in fact amounts to approximating a filter kernel by sampling. Jittering depends on the kind of descriptor parameter, for example, positions are jittered in the tangent plane of an intersection, see Algorithm 1. The resulting noise is clearly preferable over the visible discretization artifacts



Figure 5: Jittering trades quantization artifacts for noise. Left: Note that the level of detail of the jittered location (red) may differ from the one of the original location (green). Spatial jittering hides otherwise visible quantization artifacts (middle): The resulting noise (right) is more amenable to the eye and much simpler to remove by a secondary filter.

Algorithm 1: Computation of the two hashes used for lookup. Note that the arguments of a hash function, which form the descriptor, may be extended to refine clustering.

Input: Location x of the vertex, the normal n , the position of the camera p_{cam} , and the scale s .

Output: Hash i to determine the position in the hash table and hash v for verification.

$l \leftarrow \text{level_of_detail}(|p_{cam} - x|)$

$x' \leftarrow x + \text{jitter}(n) \cdot s \cdot 2^l$

$l' \leftarrow \text{level_of_detail}(|p_{cam} - x'|)$

$\tilde{x} \leftarrow \lfloor \frac{x'}{s \cdot 2^{l'}} \rfloor$

$i \leftarrow \text{hash}(\tilde{x}, \dots)$

$v \leftarrow \text{hash2}(\tilde{x}, n, \dots)$

resulting from quantization, as illustrated and shown in Figure 5. Other than discretization artifacts, noise from jitter is simple to filter.

3.3 Accumulation over Time

Accumulating contributions across frames dramatically increases efficiency. For static scenes, the averages will converge. For dynamic environments, maintaining two sets of averaged contributions and combining them with an exponential moving average $c = \alpha \cdot c_{old} + (1 - \alpha) \cdot c_{new}$ is a common tradeoff between convergence and temporal adaptivity. Big changes even for hashes with a large number of old contributions can be controlled by the parameter α .

However, combining the averages c_{old} and c_{new} by an exponential average is not equivalent to temporal integration. Especially averages of hashes with relatively few samples do not converge. In this case it may be beneficial to accumulate samples over time up to a certain degree. This may be implemented using a fixed threshold for the number of samples and accumulating samples across frames until reaching it. In the same spirit, α may depend on the number of samples, again using an upper bound to guarantee temporal responsiveness.

3.4 Eviction Strategy

Evicting contributions of hashes which have not been queried for a certain period of time is necessary for larger scenes and changing

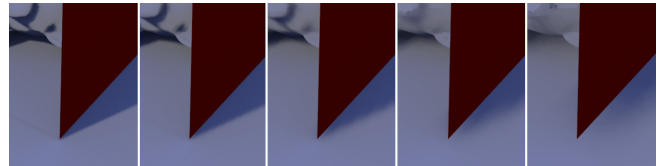


Figure 6: Increasing the filter size by lowering the quantization rate (left to right) increasingly blurs shadows and also increases the amount of light and shadow leaking.

camera. Besides the least recently used (LRU) eviction strategy, heuristics based on longer term observations are efficient.

A very simple implementation relies on replacing the most significant bits of the verification hash by a priority composed of for example vertex density and last access time during temporal filtering. Thus the pseudo-randomly hashed least significant bits guarantee missing contributions to be uniformly distributed across the scene, while the most significant bits ensure that contributions are evicted according to priority. This allows collision handling and eviction to be realized by a single atomicMin operation.

Due to camera movement or other parameters changing hashes over time, a small number of old contributions may not be found any more. While jittering may hide discontinuities due to these changes as well, it does not compensate for the significant loss in quality due to the reduced number of averaged samples. Therefore, we perform an additional neighborhood search in these rare cases. A similar issue may appear for parts of the scene that do not have many other contributions with identical hashes.

4 RESULTS AND DISCUSSION

While filtering contributions at primary intersections with the proposed algorithm is quite fast, it only removes some artifacts of filtering in screen space. However, hashed path space filtering has been designed to target real-time light transport simulation: It is the only efficient fallback when screen space filtering fails or is not available, for example, for specular or transparent objects.

Filtering on non-diffuse surfaces requires to include additional parameters in the path descriptor and heuristics such as increasing the quantization in areas with non-diffuse materials to minimize the visible artifacts.

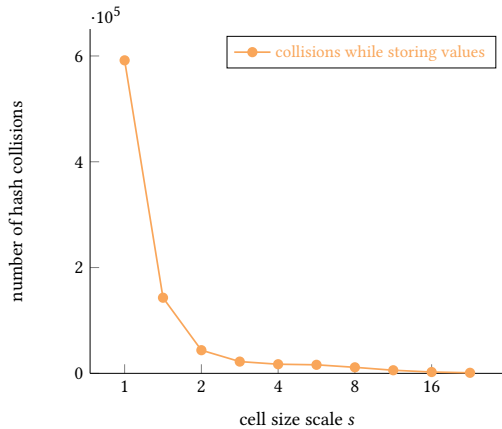


Figure 7: Average number of hash collisions for different hash table sizes.

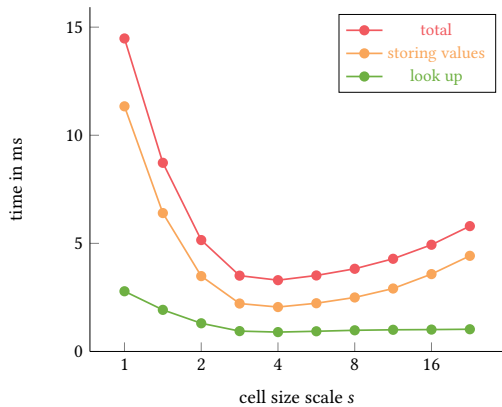


Figure 8: Time required for filtering (Quadro M6000)

Filtering, and especially accumulating contributions, is always prone to light and shadow leaking (see Figure 6), which is the price we pay for performance. Some artifacts may be ameliorated by employing suitable heuristics as reviewed in [7, Sec.2.1].

The new algorithm filters incoherent intersections at HD resolution (1920×1080 pixels) in about 3 ms on an NVIDIA Titan V GPU and in about 6 ms on an NVIDIA Titan X GPU. Filtering primary intersections doubles the performance due to the more coherent memory access patterns.

The image quality is determined by the filter size, which balances noise versus blur as shown in Figure 6. Both the number of collisions in the hash table in Figure 7 and hence the performance of filtering as shown in Figure 8 depend on the size of the voxels. The voxel size is specified by s -times the projected size of a pixel. Note that maximum performance does not necessarily coincide with best image quality. The hash table size is chosen proportional to the number of pixels at target resolution such that potentially one vertex could be stored per pixel.

While path space filtering dramatically reduces the noise at low sampling rates (see Figures 1 and 9), some noise is added back by

spatial jittering. Instead of selecting the first sufficiently diffuse vertex along a path from the camera, path space filtering can be applied at any vertex. For example, filtering at the second sufficiently diffuse vertex as shown in Figure 10 resembles final gathering or local passes [6]. Further, it is obviously also possible to filter in several vertices along the path at the same time. In fact, path space filtering trades variance reduction for controlled bias and is orthogonal to other filtering techniques. We therefore abstain from comparisons with these: Temporal anti-aliasing and complimentary noise filters in screen space are appropriate to further reduce noise [9]. A local smoothing filter [11] can even help reduce the error inherent in the approximation.

5 CONCLUSION

Relying on only a few synchronizations during accumulation, path space filtering based on hashing scales on massively parallel hardware. Queries run in constant time and neither the traversal nor the construction of a hierarchical spatial acceleration data structure is required. Hence the algorithm is currently limited by the performance of ray tracing, which takes about 70 ms per frame as compared to 1.5 ms taken by filtering.

The simplistic algorithm overcomes many restrictions of screen space filtering, does not require motion vectors, enables noise removal beyond the first intersection including specular and transparent surfaces.

The hashing scheme still bears potential for improvement. For example, important hashes could be excluded from eviction by reducing the level of detail, i.e. accumulating their contributions at a coarser level. The same would work for cells with only a few contributions. Other than selecting a level of detail by the length of the path, path differentials and variance may be used to determine the appropriate resolution.

Besides the classic applications of path space filtering [7, Sec.3] like multi-view rendering, spectral rendering, participating media, and decoupling anti-aliasing from shading, the adaptive hashing scheme can be used for photon mapping [5, 6] and irradiance probes in reinforcement learned importance sampling [3] in combination with final gathering to store radiance probes.

ACKNOWLEDGEMENTS

The authors would like to thank Petrik Clarberg for profound discussions and comments.

REFERENCES

- [1] S. Bako, T. Vogels, B. McWilliams, M. Meyer, J. Novák, A. Harvill, P. Sen, T. Deroose, and F. Rousselle. 2017. Kernel-predicting Convolutional Networks for Denoising Monte Carlo Renderings. *ACM Trans. Graph.* 36, 4, Article 97 (July 2017), 14 pages. <https://doi.org/10.1145/3072959.3073708>
- [2] C. Chaitanya, A. Kaplanyan, C. Schied, M. Salvi, A. Lefohn, D. Nowrouzezahrai, and T. Aila. 2017. Interactive Reconstruction of Monte Carlo Image Sequences Using a Recurrent Denoising Autoencoder. *ACM Trans. Graph.* 36, 4, Article 98 (July 2017), 12 pages. <https://doi.org/10.1145/3072959.3073601>
- [3] K. Dahm and A. Keller. 2017. Learning Light Transport the Reinforced Way, to appear in Monte Carlo and Quasi-Monte Carlo Methods 2016. *CoRR* abs/1701.07403 (2017). <http://arxiv.org/abs/1701.07403>
- [4] P. Gautron, M. Droske, C. Wächter, L. Kettner, A. Keller, N. Binder, and K. Dahm. 2014. Path Space Similarity Determined by Fourier Histogram Descriptors. In *ACM SIGGRAPH 2014 Talks (SIGGRAPH '14)*. ACM, New York, NY, USA, Article 39, 1 pages. <https://doi.org/10.1145/2614106.2614117>
- [5] T. Hachisuka and H. Jensen. 2009. Stochastic progressive photon mapping. In *SIGGRAPH Asia '09: ACM SIGGRAPH Asia 2009 papers*. ACM, 1–8.



Figure 9: Path tracing at one path per pixel (top) in combination with hashed path space filtering (middle) very closely approximates the reference solution (bottom) using 1024 paths per pixel and does so in about 1.5 ms in HD resolution. Unreal Engine demo by Epic Games.



Figure 10: Indirect illumination by hashed path space filtering at the second bounce: At 16 paths per pixel (left), the variance of the integrand is dramatically reduced (right).

- [6] H. Jensen. 2001. *Realistic Image Synthesis Using Photon Mapping*. AK Peters.
- [7] A. Keller, K. Dahm, and N. Binder. 2016. Path Space Filtering. In *Monte Carlo and Quasi-Monte Carlo Methods 2014*, R. Cools and D. Nuyens (Eds.). Springer, 423–436.
- [8] Amazon Lumberyard. 2017. Amazon Lumberyard Bistro, Open Research Content Archive (ORCA). <http://developer.nvidia.com/orca/amazon-lumberyard-bistro>
- [9] M. Mara, M. McGuire, B. Bitterli, and W. Jarosz. 2017. An Efficient Denoising Algorithm for Global Illumination. In *ACM SIGGRAPH / Eurographics High Performance Graphics*. 7. <http://casual-effects.com/research/Mara2017Denoise/index.html>
- [10] J. Munkberg, J. Hasselgren, P. Clarberg, M. Andersson, and T. Akenine-Möller. 2016. Texture Space Caching and Reconstruction for Ray Tracing. *ACM Trans. Graph.* 35, 6, Article 249 (Nov. 2016), 13 pages. <https://doi.org/10.1145/2980179.2982407>
- [11] C. Schied, A. Kaplanyan, C. Wyman, A. Patney, C. Chaitanya, J. Burgess, S. Liu, C. Dachsbacher, A. Lefohn, and M. Salvi. 2017. Spatiotemporal Variance-guided Filtering: Real-time Reconstruction for Path-traced Global Illumination. In *Proceedings of High Performance Graphics (HPG '17)*. ACM, New York, NY, USA, Article 2, 12 pages. <https://doi.org/10.1145/3105762.3105770>
- [12] P. Sen, M. Zwicker, F. Rousselle, S.-E. Yoon, and N. Kalantari. 2015. Denoising Your Monte Carlo Renders: Recent Advances in Image-space Adaptive Sampling and Reconstruction. In *ACM SIGGRAPH 2015 Courses (SIGGRAPH '15)*. ACM, New York, NY, USA, Article 11, 255 pages. <https://doi.org/10.1145/2776880.2792740>
- [13] M. Zwicker, W. Jarosz, J. Lehtinen, B. Moon, R. Ramamoorthi, F. Rousselle, P. Sen, C. Soler, and S.-E. Yoon. 2015. Recent Advances in Adaptive Sampling and Reconstruction for Monte Carlo Rendering. *Comput. Graph. Forum* 34, 2 (May 2015), 667–681. <https://doi.org/10.1111/cgf.12592>